CHEMISTRY OF MATERIALS

Article

pubs.acs.org/cm

Role of Amine–Cavity Interactions in Determining the Structure and Mechanical Properties of the Ferroelectric Hybrid Perovskite $[NH_3NH_2]Zn(HCOO)_3$

Gregor Kieslich,[*,†] Alexander C. Forse,[‡] Shijing Sun,[†] Keith T. Butler,[§] Shohei Kumagai,[†,∥,⊥] Yue Wu,[#] Mark R. Warren,[@] Aron Walsh,[§,▽] Clare P. Grey,[‡] and Anthony K. Cheetham[*,†]

[†]Department of Materials Science and Metallurgy, University of Cambridge, 27 Charles Babbage Road, Cambridge CB3 0FS, U.K.

[‡]Department of Chemistry, University of Cambridge, Lensfield Road, Cambridge CB2 1EW, U.K.

[§]Centre for Sustainable Chemical Technologies and Department of Chemistry, University of Bath, Bath BA2 7AY, U.K.

[∥]Department of Chemistry, Graduate School of Science, Tohoku University, 6-3 Aza-Aoba, Aramaki, Aoba-ku, Sendai 980-8578, Japan

[⊥]WPI-Advanced Institute for Materials Research, Tohoku University, 2-2-1 Katahira, Aoba-ku, Sendai 980-8577, Japan

[#]Chemistry Research Laboratory, Department of Chemistry, University of Oxford, 12 Mansfield Road, Oxford OX1 3TA, U.K.

[@]Diamond Light Source Ltd., Harwell Science & Innovation Campus, Didcot, Oxfordshire OX11 0DE, U.K.

[▽]Global E3 Institute and Department of Materials Science and Engineering, Yonsei University, Seoul 120-749, Korea

Supporting Information

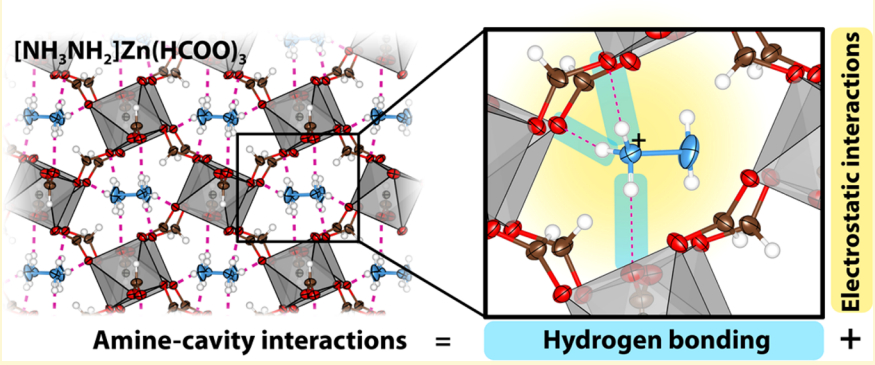

ABSTRACT: Dense formate frameworks with a perovskite-like architecture exhibit multiferroic behavior and tunable mechanical properties. In such materials, interactions between the protonated amine and the metal–formate cavity have a large impact on the mechanical properties. We use complementary single-crystal X-ray diffraction and ^{1}H solid state nuclear magnetic resonance spectroscopy to investigate amine–cavity interactions in $[NH_3NH_2]Zn(HCOO)_3$. The results suggest that these interactions can be described as salt bridges similar to those in proteins and artificially synthesized helical polymers, where ionic interactions and hydrogen bonds are present at the same time. Nanoindentation and high-pressure single-crystal X-ray diffraction were used to study the mechanical properties of $[NH_3NH_2]Zn(HCOO)_3$, yielding elastic moduli of E_{001} = 26.5 GPa and E_{110} = 24.6 GPa and a bulk modulus of K = 19 GPa. The mechanical properties suggest that, despite the relatively low packing density of $[NH_3NH_2]Zn(HCOO)_3$, the amine–cavity interactions strengthen the framework significantly in comparison with related materials.

INTRODUCTION

An understanding of crystal chemistry is the key in the design of materials with specific physical properties. Over the past decade, the development of analysis techniques and computational methods have helped in tackling this challenge and have provided insights into fascinating scientific phenomena and processes.[1−5] For purely inorganic materials, there are guidelines to explain the stability and formation of certain structural features.[6,7] In organic–inorganic hybrids, however, the range of different chemical interactions and bonds makes crystal engineering a more complex challenge.[8] Crystal packing and binding energies often compete with entropic effects, and other factors such as density and synthetic conditions take on increased importance.[9] For instance, hydrogen bonds (HBs) that are absent in classic inorganic materials have been shown to be responsible for interesting phenomena such as poly-

Received: October 26, 2015
Revised: November 25, 2015
Published: November 25, 2015

DOI: 10.1021/acs.chemmater.5b04143
Chem. Mater. 2016, 28, 312−317

morphism and glassy phase transitions in hybrid materials.[10,11] The energy of HBs usually lies in the range of 5−145 kJ mol^{-1}, and therefore, many materials show a crystal structure in which the number of possible HBs is maximized.[12]

Under these circumstances, it is not surprising that in the family of hybrid perovskites with the general formula $AmBX_3$, hydrogen bonding interactions play an important role.[13−15] In such frameworks, a divalent metal B^{2+} and an (organic) ion X^- form a pseudocubic BX_3^- (ReO_3-like) cavity while an organic cation Am^+, typically a protonated amine, is located within this cavity for charge balance.[16,17] In the family of formate perovskites, $AmB(HCOO)_3$,[18−20] the protonated amine Am^+ interacts with the metal−formate cavity through both HBs and ionic interactions, with the strengths of these interactions depending upon the molecular structure, size, and symmetry of the protonated amine. Furthermore, the protonated amine is responsible for fascinating ferroelectric-to-paraelectric phase transitions with tunable phase transition temperatures.[14] Panels a and b of Figure 1 show a schematic of the structure of $[NH_3NH_2]Zn(HCOO)_3$ with a focus on the pseudocubic unit cell and HBs.[21]

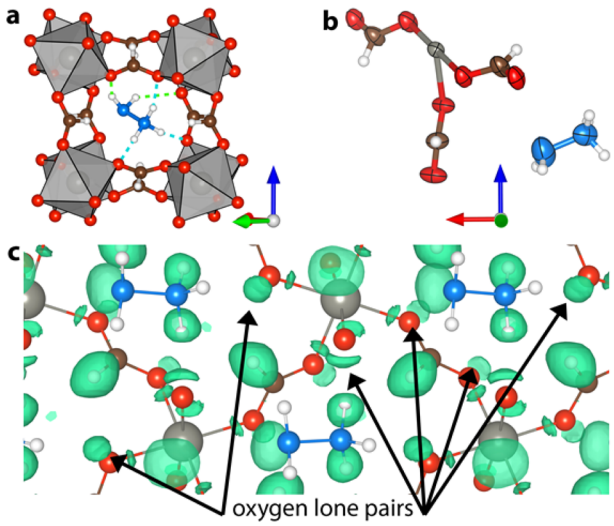

Figure 1. Schematic of the pseudocubic perovskite building block of $[NH_3NH_2]Zn(HCOO)_3$ (a) and the asymmetric unit cell (b). Light green and blue dashed lines in panel a correspond to hydrogen bonding interactions between the hydrazinium ion and the metal−formate framework. In panel b, hydrogen bonding interactions have been omitted for the sake of clarity. (c) Electron localization function (ELF) of $[NH_3NH_2)]Zn(HCOO)_3$ with an isosurface level f = 0.88 along the c-axis. In simple terms, the ELF provides a method for mapping the electron pair probability in direct space, thus allowing an analysis of the types of chemical bonding in a chemically intuitive way. In the figure, red spheres correspond to oxygen, gray spheres to zinc, brown spheres to carbon, blue spheres to nitrogen, and white spheres to hydrogen atoms.

The mechanical response of a framework is sensitive to the relative strengths of all kinds of chemical bonding. Within formate frameworks, $[C(NH_2)_3]Mn(HCOO)_3$ [$C(NH_2)_3$ = guan] is the stiffest framework reported to date,[22] with an elastic modulus of ∼26 GPa. Other $AmB(HCOO)_3$ formates, such as $[C_3N_1H_8]Mn(HCOO)_3$ ($C_3N_1H_8$ = azet) and $[(CH_3)_2NH_2]Mn(HCOO)_3$ [$(CH_3)_2NH_2$ = DMA], show smaller elastic moduli of 12 and 19 GPa, respectively, which has been ascribed to them having fewer HBs between the pronated amines and the metal−formate cavities.[22]

In nanoindentation experiments, the zinc analogue, [DMA]-$Zn(HCOO)_3$, shows mechanical properties similar to those of $[DMA]Mn(HCOO)_3$,[23] which was ascribed to the absence of ligand field stabilization energy in both compounds. On the other hand, infrared results point to a stronger Zn−formate bond that could lead to greater stiffness of the Zn-based framework.[24] This is consistent with results from Brillouin scattering on $[NH_4]M(HCOO)_3$ (M = Mn^{2+} and Zn^{2+}) and a recently published study on the thermally responsive behavior of formate frameworks, which both indicate greater stiffness for the Zn^{2+} frameworks.[25,26] Currently, this discrepancy is explained by the fact that in the case of nanoindentation experiments, a uniaxial force is applied to the crystal whereas temperature variation applies an isotropic external stimulus. Notwithstanding the correlation between the elastic moduli and the number of HBs, the effective strength of the individual hydrogen bonds is also important. At the same time, there are ionic monopolar interactions between the amine cation and the ReO_3-like cavity whose strengths mainly depend on the amine···O distances.

Despite the prominent role of the protonated amines, experimental studies that focus on amine−cavity interactions in such frameworks, e.g., by neutron diffraction and infrared (IR) spectroscopy, are still quite limited.[24,27−30] In single-crystal X-ray diffraction (SCXRD), which is the common technique for determining structure, the hydrogen positions are refined in the so-called "riding model" with fixed C−H and N−H bond lengths.[31] On the other hand, nuclear magnetic resonance (NMR) spectroscopy is emerging as a technique that can probe the precise local structure of framework materials.[32−34] For instance, Xu et al.[35] used ^{1}H NMR to distinguish between the subtly different local environments of the formate hydrogen atoms in $Mg_3(HCOO)_6$.

In this work, we obtain the accurate positions of hydrogen atoms in $[NH_3NH_2]Zn(HCOO)_3$ by a combined approach of experiment and calculations based on density functional theory (DFT). Initially, the structure is determined using SCXRD and then refined on the basis of ^{1}H MAS NMR spectroscopy data. The mechanical properties of $[NH_3NH_2]Zn(HCOO)_3$ are then determined experimentally by nanoindentation and high-pressure SCXRD and linked to the underlying structure of $[NH_3NH_2]Zn(HCOO)_3$ where the nature of the amine−cavity interactions play a major role.

RESULTS AND DISCUSSION

Chemical Bonding in $[NH_3NH_2]Zn(HCOO)_3$. Single-crystal X-ray diffraction on $[NH_3NH_2]Zn(HCOO)_3$ was performed at room temperature. The structure, bond lengths, and angles are in agreement with the structure reported by Gao et al.[21] (see SI-Figure 1, SI-Table 1, and SI-Table 2 of the Supporting Information). $[NH_3NH_2]Zn(HCOO)_3$ crystallizes in a perovskite-like framework in space group $Pna2_1$ with the following unit cell dimensions: a = 8.66793(10) Å, b = 7.74839(8) Å, and c = 11.54775(13) Å. On the basis of the structure obtained by SCXRD, several different bonding interactions can be identified: (i) covalent bonds within the formate linker, (ii) coordination bonds between the partially negatively charged oxygen and the divalent metal, (iii) ionic interactions between the ReO_3-like metal−formate cavity and the protonated amine, and (iv) hydrogen bonding interactions between hydrogen atoms of the protonated amine and the

DOI: 10.1021/acs.chemmater.5b04143
Chem. Mater. 2016, 28, 312−317

oxygen formate atoms. One way to analyze the chemical bonding from a more fundamental point of view is the calculation of the electron localization function (ELF) shown in Figure 1c, which was obtained by DFT calculations based on an extended representation of the electron density including the semicore state of Zn.[36−38]

In the context of this work, the most important features visible in the ELF are the maxima located at the oxygen atoms, highlighted in Figure 1c, which correspond to oxygen lone pairs that are crucial for amine−cavity interactions. For a discussion of other features visible in the ELF, see the Supporting Information. The lone pairs are centers of negative charge and interact with protonated amine through (i) purely ionic interactions, R′−HN^+···OR_2, and (ii) hydrogen bonds, R′−NH···OR_2. Via examination of the structure obtained from SCXRD, in $[NH_3NH_2]Zn(HCOO)_3$, the protonated nitrogen has six oxygen neighbors close in space, at distances of 2.890 Å (O2), 2.923 Å (O6), 2.941 Å (O4), 2.971 Å (O5), 3.027 Å (O3), and 3.126 Å (O1). In $[DMA]Zn(HCOO)_3$, only three nearest neighbors are present at distances between 2.834 and 3.309 Å. In the guanidinium analogue, the stiffest member of the formate family investigated to date,[22] an analysis of ionic interactions is more challenging because of the charge distribution in the guanidinium cation over four atoms. However, similar to $[NH_3NH_2]Zn(HCOO)_3$, $[guan]Mn(HCOO)_3$] has six short N···O distances between 2.953 and 2.991 Å, which together with the guanidinium cation allow for six strong HBs at the same time. The ionic interactions, on the other hand, seem to be weakened for the guanidinium formates because of the reduced charge at the nitrogen atoms. Therefore, in $[NH_3NH_2]Zn(HCOO)_3$, the ionic interactions between the nitrogen atom and the cavity seem to be stronger than in comparable formate frameworks.

Positions of Hydrogen Atoms Quantified by SCXRD, ^{1}H NMR, and First-Principles Calculations. The ^{1}H magic angle spinning (MAS) NMR spectrum of $[NH_3NH_2]Zn(HCOO)_3$ was recorded with an MAS rate of 60 kHz at room temperature, leading to an estimated sample temperature of ∼320 K due to frictional heating. The spectrum reveals three main signals (Figure 2a). The resolution of the NMR spectrum is strongly dependent on the MAS spinning frequency (SI-Figure 3), such that a fast MAS rate of 60 kHz was required to resolve the three proton sites. On the basis of the chemical shifts of the resonances, as well as a two-dimensional heteronuclear correlation (HETCOR) experiment (SI-Figure 4), which reveals a correlation between the ^{13}C and ^{1}H nuclei of the formate groups (as these are close in space), we assign the signals at δ ^{1}H 8.3 ppm to the formate hydrogen atoms, those at δ ^{1}H = 9.2 ppm to the NH_3 group hydrogens, and the signals at δ ^{1}H = 4.0 ppm to NH_2 group hydrogens. The integrated intensities of 1:1.05:0.61 are in good agreement with the expected ratio of 1:1:0.67.

To explore these results more thoroughly, ^{1}H NMR chemical shifts were calculated using first-principles DFT calculations in CASTEP.[39] Initially, the chemical shifts were calculated from the structure determined from SCXRD, but here the agreement between the calculated and experimental shifts is very poor (see Table 1 and the simulated spectrum in Figure 2b). In particular, the calculated chemical shifts of the NH_3 and NH_2 groups are significantly smaller than the experimental values, indicating that the positions of the hydrogen atoms are inaccurate in the structure determined by SCXRD. The geometry of the structure was then optimized in CASTEP while constraining

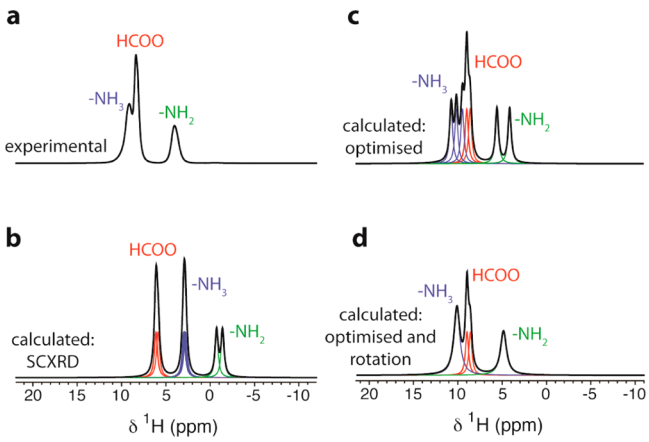

Figure 2. Experimental (a) and simulated ^{1}H MAS NMR spectra for $[NH_3NH_2]Zn(HCOO)_3$. Spectra were simulated for the NMR parameters calculated for both the SCXRD structure (b) and the structure obtained from geometry optimization in CASTEP (c). For the simulations on the optimized structure, an additional simulation is shown using the averaged NH_3 and NH_2 shifts, representing the rapid rotation of the NH_3 and NH_2 groups (d). Here, 400 Hz line broadening was added to the NH_3 and NH_2 resonances. In all other cases, the simulated line broadening was 200 Hz.

Table 1. Experimental and Calculated ^{1}H Chemical Shifts of $[NH_3NH_2]Zn(HCOO)_3$[a]

	δ ^{1}H (ppm)		
	$HCOO^-$	NH_3^+	NH_2
calculated (SCXRD)	6.1	2.9	−1.0
calculated (optimized)	8.9	10.1	4.9
experimental	8.3	9.2	4.0

[a]Calculated values are given for the SCXRD structure, as well as for the structure obtained from geometry optimization in CASTEP.

the space group and the lattice parameters. The chemical shifts calculated for the optimized structure show much better agreement with the experimental values (Table 1 and Figure 2c), with the average values agreeing within 1 ppm. In contrast to the calculated NMR parameters (at 0 K, with no dynamic effects included), distinct resonances are not experimentally observed for the individual hydrogen atoms in the NH_2 and NH_3 groups (Figure 2). This suggests that there is rapid rotation of the NH_3 and NH_2 groups, resulting in an averaging of the chemical shifts. Note here that it is not possible to distinguish between rotation of the whole molecule and separate rotations of the NH_3 and NH_2 groups. Indeed, the experimental spectrum was well reproduced by simulating spectra using the average NH_3 and NH_2 shifts, with line broadening added (Figure 3d). On the basis of the calculated NMR parameters, and assuming coalescence of the resonances due to rotation, we estimate a lower limit for the frequency of rotation of these groups of 700 Hz.

On the basis of the geometry-optimized structure of $[NH_3NH_2]Zn(HCOO)_3$, N−H···O distances can be determined and, in turn, the strengths of the HBs can be evaluated. In Table 2, final N−H and N−H···O bond lengths and angles of the optimized crystal structure are given. The distances obtained for the N−H···O bond lengths of the NH_3 group, 1.780−1.739 Å, are considered to be moderate to strong HBs in the literature.[12] The large N−H···O bond angles of 161.33−169.09° are in agreement with this. The HBs at the NH_2 group

DOI: 10.1021/acs.chemmater.5b04143
Chem. Mater. 2016, 28, 312−317

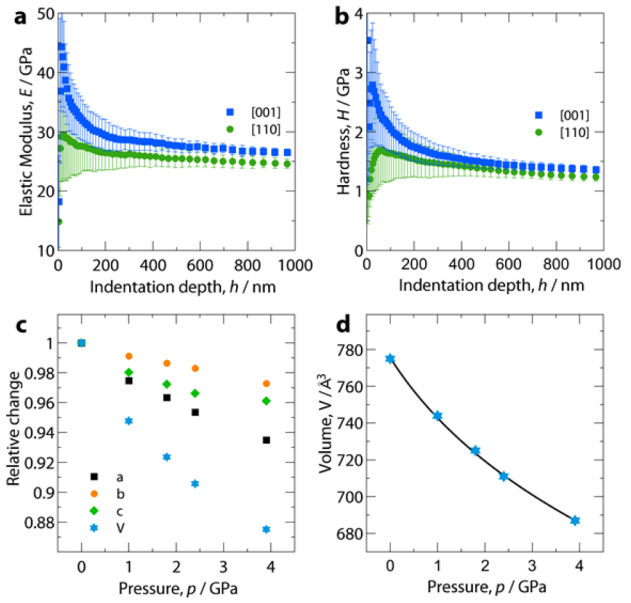

Figure 3. Elastic moduli (a) and hardnesses (b) as a function of indentation depth along [001] (blue) and [110] (green) in $[NH_3NH_2]Zn(HCOO)_3$. The elastic moduli are similar to those of $[guan]Mn(HCOO)_3$, the stiffest formate framework reported so far.[22] For the corresponding load−displacement curve, see SI-Figure 5. In panels c and d, the evolution of lattice parameters and volume with pressure of $[NH_3NH_2]Zn(HCOO)_3$ is shown. The black fitting curve in panel d corresponds to a third-order Burch−Murnaghan fit leading to a bulk modulus of $K = 19 \pm 2$ GPa.

Table 2. N−H and N−H···O Bond Lengths and Angles in the Optimized Structure of $[NH_3NH_2]Zn(HCOO)_3$

	N−H (Å)	N−H···O (Å)/angle (deg)
NH_3	1.058	1.780/167.65
	1.055	1.874/161.33
	1.053	1.817/169.09
NH_2	1.035	2.195/139.88
	1.037	2.023/148.12

are weaker, indicated by longer N−H···O distances and smaller angles of 139.88° and 148.12°. Therefore, all five hydrogen atoms are involved in HBs. Taken together with the ionic interactions discussed earlier, amine−cavity interactions of the NH_3 group and the metal−formate cavity can be compared to salt bridges in proteins and artificially synthesized helical polymers.[40] In general, salt bridges play an important role in determining the three-dimensional structure of various materials. For instance, in proteins, entropically unfavorable conformations can be stabilized, emphasizing the energy gain involved in this interaction.

Elastic Moduli, Hardness, and Bulk Modulus of $[NH_3NH_2]Zn(HCOO)_3$. The mechanical properties of $[NH_3NH_2]Zn(HCOO)_3$ single crystals were studied using nanoindentation and high-pressure SCXRD (see Figure 3). Nanoindentation experiments were performed along [001] and [110] $[NH_3NH_2]Zn(HCOO)_3$ single crystals with a size of ∼1 mm (see the methods of the Supporting Information for details). The elastic moduli were found to be $E_{001} = 26.5$ GPa and $E_{110} = 24.5$ GPa, which means it is comparable to the stiffest $[guan]Mn(HCOO)_3$ perovskite-like framework to date, $E_{010} = 28.6$ GPa and $E_{101} = 24.5$ GPa. The hardnesses $H_{001} = 1.36$ GPa and $H_{110} = 1.24$ GPa also reflect the high stiffness of the framework [for $[guan]Mn(HCOO)_3$, $H_{010} = 1.25$ GPa and $H_{101} = 1.18$ GPa]. The macroscopic hardness of a material is generally characterized by strong intermolecular bonds, thus confirming the stiff nature of the framework suggested by strong amine−cavity interactions.

Because of their similar mechanical properties, it is worth comparing compounds $[NH_3NH_2]Zn(HCOO)_3$ and $[guan]Mn(HCOO)_3$. Neither framework has a contribution from ligand field stabilization energy, though different ionic sizes of the metal ions suggest different bond characteristics and strengths.[41] Furthermore, the influence of physical density on the mechanical properties seems to be important only when comparing different types of hybrid materials, e.g., highly porous MOFs ($\rho \approx 0.9$−1.5 g cm^{-3}; $E < 10$ GPa) and dense MOFs ($\rho \geq 2$ g cm^{-3}; $E > 10$ GPa). At the same time, the influence of relative packing density on the stiffness of the frameworks, indicated by different tolerance factors (TFs), appears to be negligible when the divalent metal is varied.[23] This is expected as the TF concept has to be seen as a guideline, and small distortions of the framework, for instance, octahedral tilting due to varying metal radii, are not considered in TFs. On the other hand, changing the protonated amine has a large impact and must be considered in our discussion. We therefore identify three main factors influencing the stiffness: (i) the amine−cavity interactions, (ii) the relative packing density, and (iii) variation of stiffness related to the different metal−formate bond strengths. With regard to the metal−formate bond strength, so far only minor differences in the hardness of Zn- and Mn-based compounds have been detected in nanoindentation experiments. These point to a slightly stronger Zn−formate bond,[23] which is in agreement with the results of IR experiments. Differences in the elastic moduli have not been observed so far. On the other hand, the relative packing densities as given by the TFs indicate a more densely packed framework for $[guan]Mn(HCOO)_3$ ($TF_{[NH_2NH_3]Zn} = 0.839$, and $TF_{[guan]Mn} = 0.955$), which would lead to a stiffer $[guan]Mn(HCOO)_3$ network.[42] On the basis of these considerations, we believe that amine−cavity interactions in $[NH_3NH_2]Zn(HCOO)_3$ seem to be equal if not stronger than in $[guan]Mn(HCOO)_3$, which confirms the salt bridge-like behavior discussed above.

To complete the characterization of the mechanical properties, high-pressure SCXRD was performed using synchrotron radiation [$\lambda = 0.6889$ Å (Figure 3c,d)]. The experiment was performed in a diamond anvil cell setup using Fluorinert70 (FC-70) as the pressure-transmitting medium. Although the data sets were not sufficient for structure refinement, lattice parameters up to a pressure of 4 GPa could be extracted. During indexing, no evidence of a pressure-induced phase transition was observed and the dependency of lattice parameters and volume on pressure is shown in panels c and d of Figure 3. By using a third-order Birch−Murnaghan equation of state,[43,44] a bulk modulus of $K = 19 \pm 2$ GPa was obtained. This value is consistent with experimental values obtained for other formate and dense hybrid frameworks, such as the dense ferroelectric $[NH_4]Zn(HCOO)_3$ ($K = 32.8$ GPa);[13] note that $[NH_4]Zn(HCOO)_3$ crystallizes in a chiral structure with $[NH_4]^+$ in hexagonal channels, and not in a perovskite-like framework.

DOI: 10.1021/acs.chemmater.5b04143
Chem. Mater. 2016, 28, 312−317

CONCLUSIONS

In conclusion, we have presented a thorough analysis of the chemical bonding in the $AmBX_3$ formate metal−organic framework $[NH_3NH_2]Zn(HCOO)_3$ and linked our findings to the mechanical properties determined by nanoindentation and high-pressure SCXRD. The insights gained in this work are important not only from a fundamental point of view but also for further studies regarding the tuning of the ferroelectric properties of formate frameworks in general. By combining complementary SCXRD and ^1H MAS NMR with computational studies, we precisely determined the locations of the hydrogen atoms. We found that lone pairs located at oxygen atoms in the metal−formate cavity atoms are involved in salt bridge-like interactions with the NH_3 group of $[NH_3NH_2]^+$, with both ionic and hydrogen bonding interactions present. The NH_2 group forms a further two HBs, leading to five moderate to strong HBs in $[NH_3NH_2]Zn(HCOO)_3$. The strong amine−cavity interactions result in a stiff lattice with elastic moduli of E_{001} = 26.5 GPa and E_{110} = 24.6 GPa, hardnesses of H_{001} = 1.36 GPa and H_{110} = 1.24 GPa, and a bulk modulus of K = 19 GPa. The salt bridge-like interactions found for the NH_3 group seem to be unique in $[NH_3NH_2]^+$, highlighting the influence of molecular structure and size on the strength of amine−cavity interactions. Our study gives an experimental attempt to understand amine−cavity interactions on a molecular level and underlines the importance of using complementary experimental techniques to reveal structure−property relationships on a molecular scale.

ASSOCIATED CONTENT

Supporting Information

The Supporting Information is available free of charge on the ACS Publications website at DOI: 10.1021/acs.chemmater.5b04143.

Details of the structure solution (SI-Figure 1 and SI-Tables 1 and 2), the ELF (SI-Figure 2), ^1H MAS NMR experiments (SI-Figures 3 and 4), nanoindentation experiments (SI-Figure 5), and all experimental procedures related to this work (PDF)

AUTHOR INFORMATION

Corresponding Authors

*E-mail: gk354@cam.ac.uk.
*E-mail: akc30@cam.ac.uk.

Notes

The authors declare no competing financial interest.

ACKNOWLEDGMENTS

G.K. is the holder of a postdoctoral fellowship granted by the Deutsche Forschungsgemeinschaft (KI1879). A.C.F. acknowledges the Sims Scholarship for funding. S.S. thanks the Cambridge Overseas Trust for support. Calculations in CASTEP were performed using the Darwin Supercomputer of the University of Cambridge High Performance Computing Service (http://www.hpc.cam.ac.uk/), provided by Dell Inc. using Strategic Research Infrastructure Funding from the Higher Education Funding Council for England and funding from the Science and Technology Facilities Council. Y.W. acknowledges EU FP7 Grant Agreement FP7-NMP4-LA-2012-280983, SHYMAN, for funding. We also thank Dave Allan at DLS beamline I19 for his help in obtaining high-pressure SCXRD data (experiment MT10184). K.T.B. is funded by EPSRC Grant EP/M009580/1. A.W. acknowledges support from ERC Starting Grant 277757. Access to the ARCHER supercomputer was facilitated through membership of the HPC Materials Chemistry Consortium (EP/F067496). We thank John Griffin for help with the NMR calculations and experiments.

REFERENCES

(1) Liu, H.; Strobridge, F. C.; Borkiewicz, O. J.; Wiaderek, K. M.; Chapman, K. W.; Chupas, P. J.; Grey, C. P. Capturing metastable structures during high-rate cycling of $LiFePO_4$ nanoparticle electrodes. *Science* **2014**, *344*, 1252817.

(2) Griffin, J. M.; Forse, A. C.; Tsai, W.-Y.; Taberna, P.-L.; Simon, P.; Grey, C. P. In situ NMR and electrochemical quartz crystal microbalance techniques reveal the structure of the electrical double layer in supercapacitors. *Nat. Mater.* **2015**, *14*, 812−819.

(3) Sideris, P. J.; Nielsen, U. G.; Gan, Z.; Grey, C. P. Mg/Al Ordering in Layered Double Hydroxides Revealed by Multinuclear NMR Spectroscopy. *Science* **2008**, *321*, 113−117.

(4) Zhang, N.; Yokota, H.; Glazer, A. M.; Ren, Z.; Keen, D. A.; Keeble, D. S.; Thomas, P. A.; Ye, Z.-G. The missing boundary in the phase diagram of $PbZr_{1-x}TixO_3$. *Nat. Commun.* **2014**, *5*, 5231.

(5) McDonald, T. M.; Mason, J. A.; Kong, X.; Bloch, E. D.; Gygi, D.; Dani, A.; Crocellà, V.; Giordanino, F.; Odoh, S. O.; Drisdell, W. S.; Vlaisavljevich, B.; Dzubak, A. L.; Poloni, R.; Schnell, S. K.; Planas, N.; Lee, K.; Pascal, T.; Wan, L. F.; Prendergast, D.; Neaton, J. B.; Smit, B.; Kortright, J. B.; Gagliardi, L.; Bordiga, S.; Reimer, J. A.; Long, J. R. Cooperative insertion of CO_2 in diamine-appended metal-organic frameworks. *Nature* **2015**, *519*, 303−308.

(6) Pauling, L. The principles determining the structure of complex ionic crystals. *J. Am. Chem. Soc.* **1929**, *51*, 1010−1026.

(7) Goldschmidt, V. M. Die Gesetze der Krystallochemie. *Naturwissenschaften* **1926**, *14*, 477−485.

(8) Cheetham, A. K.; Rao, C. N. R.; Feller, R. K. Structural diversity and chemical trends in hybrid inorganic-organic framework materials. *Chem. Commun.* **2006**, 4780.

(9) Forster, P. M.; Burbank, A. R.; Livage, C.; Férey, G.; Cheetham, A. K. The role of temperature in the synthesis of hybrid inorganic-organic materials: the example of cobalt succinates. *Chem. Commun.* **2004**, 368.

(10) Kieslich, G.; Kumagai, S.; Butler, K. T.; Okamura, T.; Hendon, C. H.; Sun, S.; Yamashita, M.; Walsh, A.; Cheetham, A. K. Role of entropic effects in controlling the polymorphism in formate ABX_3 metal-organic frameworks. *Chem. Commun.* **2015**, *51*, 15538.

(11) Besara, T.; Jain, P.; Dalal, N. S.; Kuhns, P. L.; Reyes, A. P.; Kroto, H. W.; Cheetham, A. K. Mechanism of the order-disorder phase transition, and glassy behavior in the metal-organic framework $[(CH_3)_2NH_2]Zn(HCOO)_3$. *Proc. Natl. Acad. Sci. U. S. A.* **2011**, *108*, 6828−6832.

(12) Steiner, T. The Hydrogen Bond in the Solid State. *Angew. Chem., Int. Ed.* **2002**, *41*, 48−76.

(13) Li, W.; Probert, M. R.; Kosa, M.; Bennett, T. D.; Thirumurugan, A.; Burwood, R. P.; Parinello, M.; Howard, J. A. K.; Cheetham, A. K. Negative Linear Compressibility of a Metal−Organic Framework. *J. Am. Chem. Soc.* **2012**, *134*, 11940−11943.

(14) Chen, S.; Shang, R.; Wang, B.-W.; Wang, Z.-M.; Gao, S. An A-Site Mixed-Ammonium Solid Solution Perovskite Series of $[(NH_2NH_3)_x(CH_3NH_3)_{1-x}][Mn(HCOO)_3]$ (x = 1.00−0.67). *Angew. Chem., Int. Ed.* **2015**, *54*, 11093−11096.

(15) Lee, J.-H.; Bristowe, N. C.; Bristowe, P. D.; Cheetham, A. K. Role of hydrogen-bonding and its interplay with octahedral tilting in $CH_3NH_3PbI_3$. *Chem. Commun.* **2015**, *51*, 6434−6437.

(16) Weber, D. $CH_3NH_3PbX_3$, ein Pb(II)-System mit kubischer Perowskitstruktur. *Z. Naturforsch., B: J. Chem. Sci.* **1978**, *33b*, 1443−1445.

DOI: 10.1021/acs.chemmater.5b04143
Chem. Mater. 2016, 28, 312−317

(17) Mautner, F. A.; Cortés, R.; Lezama, L.; Rojo, T. $[N(CH_3)_4][Mn(N_3)_3]$: A Compound with a Distorted Perovskite Structure through Azido Ligands. *Angew. Chem., Int. Ed. Engl.* **1996**, *35*, 78−80.
(18) Wang, Z.; Zhang, B.; Otsuka, T.; Inoue, K.; Kobayashi, H.; Kurmoo, M. Anionic NaCl-type frameworks of $[Mn^{II}(HCOO)_3^-]$, templated by alkylammonium, exhibit weak ferromagnetism. *Dalton Trans.* **2004**, 2209.
(19) Hu, K.-L.; Kurmoo, M.; Wang, Z.; Gao, S. *Chem. - Eur. J.* **2009**, *15*, 12050−12064.
(20) Wang, Z.; Hu, K.; Gao, S.; Kobayashi, H. Formate-Based Magnetic Metal-Organic Frameworks Templated by Protonated Amines. *Adv. Mater.* **2010**, *22*, 1526−1533.
(21) Chen, S.; Shang, R.; Hu, K.-L.; Wang, Z.-M.; Gao, S. $[NH_2NH_3][M(HCOO)_3]$ (M = Mn^{2+}, Zn^{2+}, Co^{2+} and Mg^{2+}. *Inorg. Chem. Front.* **2014**, *1*, 83−98.
(22) Li, W.; Thirumurugan, A.; Barton, P. T.; Lin, Z.; Henke, S.; Yeung, H. H.-M.; Wharmby, M. T.; Bithell, E. G.; Howard, C. J.; Cheetham, A. K. Mechanical Tunability via Hydrogen Bonding in Metal−Organic Frameworks with the Perovskite Architecture. *J. Am. Chem. Soc.* **2014**, *136*, 7801−7804.
(23) Tan, J.-C.; Jain, P.; Cheetham, A. K. Influence of ligand field stabilization energy on the elastic properties of multiferroic MOFs with the perovskite architecture. *Dalton Trans.* **2012**, *41*, 3949.
(24) Mączka, M.; Szymborska-Małek, K.; Ciupa, A.; Hanuza, J. Comparative studies of vibrational properties and phase transitions in metal-organic frameworks of $[NH_4][M(HCOO)_3]$ with M = Mg, Zn, Ni, Fe, Mn. *Vib. Spectrosc.* **2015**, *77*, 17−24.
(25) Mączka, M.; Ptak, M.; Kojima, S. Brillouin scattering study of ferroelectric transition mechanism in multiferroic metal-organic frameworks of $[NH_4][Mn(HCOO)_3]$ and $[NH_4][Zn(HCOO)_3]$. *Appl. Phys. Lett.* **2014**, *104*, 222903.
(26) Collings, I. E.; Hill, J. A.; Cairns, A. B.; Cooper, R. I.; Thompson, A. L.; Parker, J. E.; Tang, C. C.; Goodwin, A. L. Compositional dependence of anomalous thermal expansion in perovskite-like ABX_3 formates. *Dalton Trans.* **2015**, DOI: 10.1039/C5DT03263F.
(27) Mączka, M.; Gągor, A.; Macalik, B.; Pikul, A.; Ptak, M.; Hanuza, J. Order−Disorder Transition and Weak Ferromagnetism in the Perovskite Metal Formate Frameworks of $[(CH_3)_2NH_2][M(HCOO)_3]$ and $[(CH_3)_2ND_2][M(HCOO)_3]$ (M = Ni, Mn). *Inorg. Chem.* **2014**, *53*, 457−467.
(28) Mączka, M.; Pietraszko, A.; Macalik, B.; Hermanowicz, K. Structure, Phonon Properties, and Order−Disorder Transition in the Metal Formate Framework of $[NH_4][Mg(HCOO)_3]$. *Inorg. Chem.* **2014**, *53*, 787−794.
(29) Lawler, J. M. M.; Manuel, P.; Thompson, A. L.; Saines, P. J. Probing ferroic transitions in a multiferroic framework family: a neutron diffraction study of the ammonium transition metal formates. *Dalton Trans.* **2015**, *44*, 11613−11620.
(30) Di Sante, D.; Stroppa, A.; Jain, P.; Picozzi, S. Tuning the Ferroelectric Polarization in a Multiferroic Metal−Organic Framework. *J. Am. Chem. Soc.* **2013**, *135*, 18126−18130.
(31) Müller, P.; Herbst-Irmer, R.; Spek, A. L.; Schneider, T. R.; Sawaya, M. R. *Crystal Structure Refinement: A Crystallographer's Guide to SHELXL*; Oxford Science Publications: New York, 2006.
(32) Kong, X.; Deng, H.; Yan, F.; Kim, J.; Swisher, J. A.; Smit, B.; Yaghi, O. M.; Reimer, J. A. Mapping of Functional Groups in Metal-Organic Frameworks. *Science* **2013**, *341*, 882−885.
(33) Hoffmann, H.; Debowski, M.; Müller, P.; Paasch, S.; Senkovska, I.; Kaskel, S.; Brunner, E. Solid-State NMR Spectroscopy of Metal−Organic Framework Compounds (MOFs). *Materials* **2012**, *5*, 2537−2572.
(34) Devautour-Vinot, S.; Maurin, G.; Serre, C.; Horcajada, P.; Paula da Cunha, D.; Guillerm, V.; de Souza Costa, E.; Taulelle, F.; Martineau, C. Structure and Dynamics of the Functionalized MOF Type UiO-66(Zr): NMR and Dielectric Relaxation Spectroscopies Coupled with DFT Calculations. *Chem. Mater.* **2012**, *24*, 2168−2177.
(35) Xu, J.; Terskikh, V. V.; Chu, Y.; Zheng, A.; Huang, Y. Mapping Out Chemically Similar, Crystallographically Nonequivalent Hydrogen Sites in Metal−Organic Frameworks by ^1H Solid-State NMR Spectroscopy. *Chem. Mater.* **2015**, *27*, 3306−3316.
(36) Becke, A. D.; Edgecombe, K. E. A simple measure of electron localization in atomic and molecular systems. *J. Chem. Phys.* **1990**, *92*, 5397.
(37) Silvi, B.; Savin, A. Classification of chemical bonds based on topological analysis of electron localization functions. *Nature* **1994**, *371*, 683−686.
(38) Grin, Y.; Savin, A.; Silvi, B. In *The Chemical Bond*; Frenking, G., Shaik, S., Eds.; Wiley-VCH Verlag GmbH & Co. KGaA: Weinheim, Germany, 2014.
(39) Clark, S. J.; Segall, M. D.; Pickard, C. J.; Hasnip, P. J.; Probert, M. I. J.; Refson, K.; Payne, M. C. First principles methods using CASTEP. *Z. Kristallogr. - Cryst. Mater.* **2005**, *220*, 576−570.
(40) Kumar, S.; Nussinov, R. Close-Range Electrostatic Interactions in Proteins. *ChemBioChem* **2002**, *3*, 604.
(41) Kosa, M.; Major, D. T. Structural trends in hybrid perovskites $[Me_2NH_2]M[HCOO]_3$. *CrystEngComm* **2015**, *17*, 295−298.
(42) Kieslich, G.; Sun, S.; Cheetham, A. K. An extended Tolerance Factor approach for organic−inorganic perovskites. *Chem. Sci.* **2015**, *6*, 3430−3433.
(43) Murnaghan, F. D. The Compressibility of Media under Extreme Pressures. *Proc. Natl. Acad. Sci. U. S. A.* **1944**, *30*, 244−247.
(44) Angel, R. J.; Alvaro, M.; Gonzalez-Platas, J. EosFit7c and a Fortran module (library) for equation of state calculations. *Z. Kristallogr. - Cryst. Mater.* **2014**, *229*, 405−419.

DOI: 10.1021/acs.chemmater.5b04143
Chem. Mater. 2016, 28, 312−317